SLAC – PUB – 5391
December 1990
E

THE STATUS OF STRANGE MESON SPECTROSCOPY*

W. DUNWOODIE

Stanford Linear Accelerator Center, P.O. Box 4349, Stanford, California 94309, U.S.A.

The present status of strange meson spectroscopy is reviewed with emphasis on the results obtained with the LASS spectrometer at SLAC. The systematics of the level structure are discussed with respect to quark model expectations, and the impact of the proposed KAON Factory on the future of the subject considered.

1. INTRODUCTION

This paper presents a brief review of the status of strange meson spectroscopy. In section 2, after some initial remarks concerning spectroscopic notation and terminology, the experimental results relevant to the level structure are summarized and the main sources of information briefly discussed. The contributions from LASS are presented in greater detail in section 3, since they represent the only recent new information on the subject. In section 4, the systematics of the level structure are considered. Finally, section 5 contains concluding remarks together with some comments on the future of the subject.

2. STATUS OF THE SPECTROSCOPY

A principal objective in studying meson spectroscopy is the precise definition of the level structure of the anticipated $q\bar{q}$ meson states. In this regard, the strange sector is particularly favored since it is free, not only from the need for isoscalar-isovector separation, but also from confusion resulting from the possible production of e.g. $K\overline{K}$ molecule and/or glueball states. The light quark level structure is related to the nature of the long-range (i.e.confining) part of the $q\bar{q}$ interaction, and thus, in principle, provides information on non-perturbative QCD. In practice, it enables us to learn about QCD potential models incorporating relativistic corrections.[1]

The quark model level diagram is expected to take the form[2] illustrated qualitatively in Figure 1 for the charmonium states.[3] Here S and L denote total quark

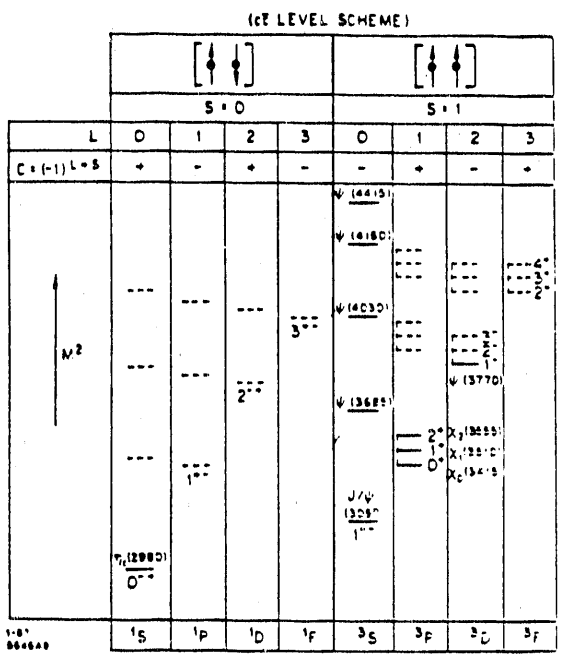

FIGURE 1
The quark model level diagram for the charmonium states; the mass scale is only qualitative.

* Work supported in part by the Department of Energy under contract No. DE-AC03-76SF00515; the National Science Foundation under grant Nos. PHY82-09144, PHY85-13808, and the Japan U.S. Cooperative Research Project on High Energy Physics.

Invited talk presented at the Rheinfels Workshop 1990 on Hadron Mass Spectrum. St. Goar, Germany, September 3-6, 1990

spin and orbital angular momentum, respectively, and C indicates the charge conjugation parity of the resulting meson state. The para-charmonium levels are singlets, whereas the ortho-charmonium levels, other than ^{3}S, are triplets separated in mass due to spin-orbit interaction. Within each column, the lowest-lying state is the ground state, and the higher states correspond to radial excitations of this state. By convention, the leading orbital excitations are the ground states with largest total angular momentum, J, and, for the triplet levels, the remaining states are termed the underlying states. In $e^+ e^-$ collisions, the ^{3}S tower of states is readily accessible, while information on the leading orbital excitations with $J \geq 3$ is lacking, and that on the corresponding underlying states is sparse. Results of a complementary nature are obtained from hadronic interaction experiments, where production of the leading orbital states predominates, and precise information on the underlying and radially-excited states requires careful amplitude analyses of high statistics data.

A somewhat optimistic summary of the observed $q\bar{q}$ levels in the strange meson sector is presented in Figure 2. This includes results from the LASS experiment, together with information derived from analyses of the charged $K\pi\pi$, $K\phi$, $K\omega$ and $\Lambda\bar{p}/\bar{\Lambda}p$ systems.[3] Of the unnatural parity levels with J^P other than 0^-, only the $J^P = 1^+$ ground state has been resolved into the states corresponding to different quark total spin; consequently, the remaining such entries in the left and right halves of Figure 2 are identical. The second radial excitation in the 0^- tower is shown as a dashed line since, of the two experiments analyzing $K\phi$,[4,5] only one finds a significant 0^- amplitude.[4]

An amplitude analysis of the $\Lambda\bar{p}/\bar{\Lambda}p$ systems[6] has yielded evidence for 2^-, 3^+ and 4^- states in the mass range 2.2-2.5 GeV/c^2; corroboration of the 2^- and 3^+ states has been obtained from other experiments.[7,8] In terms of the level diagram of Figure 2, the $K_2(2250)$ and $K_3(2320)$ are most probably radially excited states, while the $K_4(2500)$ is likely to belong to the ^{3}G ground state triplet.

Analyses of the diffractively-produced $K\phi$ system[4,5] suggest the presence of 1^+, 2^- and, as mentioned above, perhaps 0^- signals in the 1.7-1.8 GeV/c^2 mass region. The 1^+ state is a radial excitation, while the 2^- state is the $K_2(1770)$ which belongs to the ^{3}D ground state triplet.

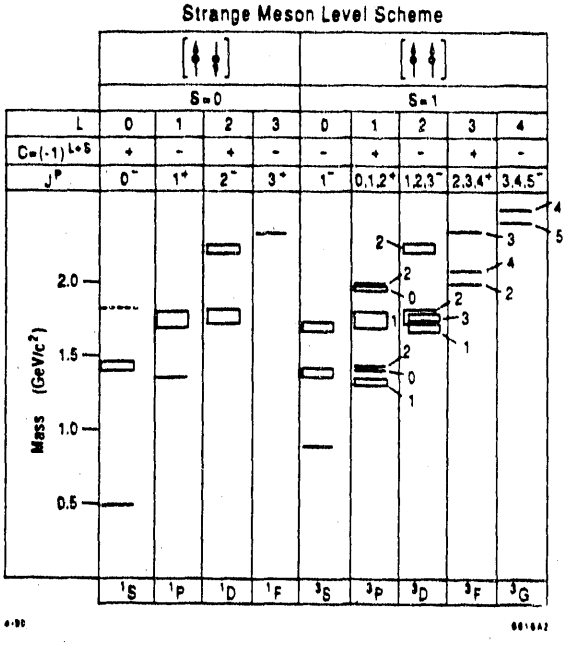

FIGURE 2
The quark model level diagram summarizing the status of strange meson spectroscopy; the C parity is that of the neutral, non-strange members of the relevant SU(3) multiplet.

The $K\omega$ system has been studied only with low statistics,[9,10] however the LASS collaboration is presently analyzing a data sample consisting of $\sim$ 120,000 events; the corresponding $K\omega$ mass distribution is shown in Figure 3. Preliminary results indicate that the low-mass peak is mainly 1^+ with some 2^+, and that the bump at $\sim$ 1.75 GeV/c^2 is made up of 1^+, 2^- and 3^- contributions.

The diffractively-produced charged $K\pi\pi$ system has been studied in detail in two large experiments.[11,10] The mass spectrum is qualitatively similar to that of Figure 3, and, although the amplitude content is somewhat the same, there are significant differences. Firstly, the low-mass 1^+ structure is resolved into two states, the $K_1(1270)$ and the $K_1(1400)$, which are further shown to be superpositions of the underlying $q\bar{q}$ states; it is these underlying states which are plotted in Figure 2.

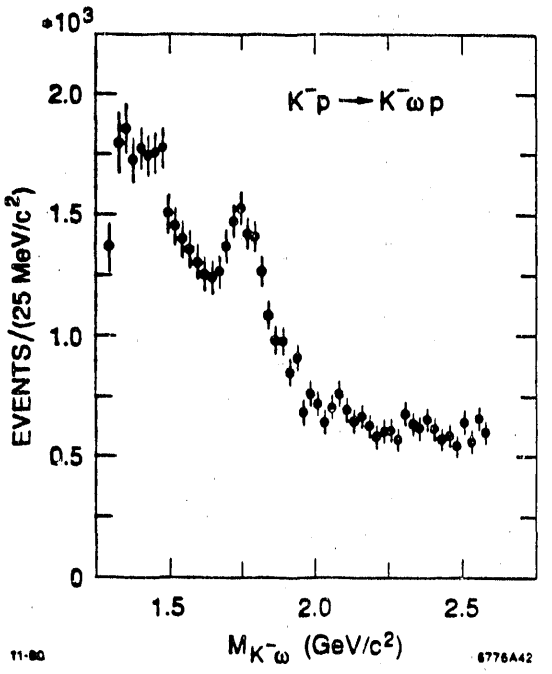

FIGURE 3
The $K^-\omega$ mass distribution from the reaction $K^-p \to K^-\omega\, p$ measured with the LASS spectrometer.

Secondly, the $K\pi\pi$ system contains a significant 0^- amplitude centered at $\sim$ 1.4 GeV/c^2; the corresponding state is interpreted as the first radial excitation of the K meson. Finally, the $K\pi\pi$ analyses yield no evidence for 3^- production in the 1.75 GeV/c^2 region, although the LASS analyses described in the next section indicate that such a contribution must be present.

The additional information from the LASS experiment on the natural parity strange meson (i.e.K^*) states shown in Figure 2 will be discussed in the next section.

3. CONTRIBUTIONS FROM LASS

This section summarizes the results on strange meson spectroscopy obtained from an exposure of the Large Aperture Superconducting Solenoid (LASS) spectrometer at SLAC to a K^- beam of 11 GeV/c. The spectrometer and relevant experimental details are described elsewhere.[12,13] The raw data sample contains $\sim$ 113 million triggers, and the resulting useful beam flux corresponds to a sensitivity of 4.1 events/nb. The acceptance is approximately uniform over almost the full 4π solid angle. The results relevant to K^* spectroscopy in the present experiment are obtained from amplitude analyses of the $\overline{K}^0\pi^+\pi^-$ system in the reaction

$$K^-p \to \overline{K}^0\pi^+\pi^-n \qquad (1)$$

and of the $K^-\pi^+$, $\overline{K}^0\pi^-$ and $K^-\eta$ systems produced in the reactions

$$K^-p \to K^-\pi^+n \qquad (2)$$

$$K^-p \to \overline{K}^0\pi^-p \qquad (3)$$

and

$$K^-p \to K^-\eta\, p\ ; \qquad (4)$$

these analyses are discussed in detail in refs. 14-17 respectively, and so only the main features will be summarized here.

The analysis of reaction (1)[14] yields the intensity distributions of Figure 4 for the natural spin-parity (J^P) states of the $\overline{K}^0\pi^+\pi^-$ system. Signals corresponding to

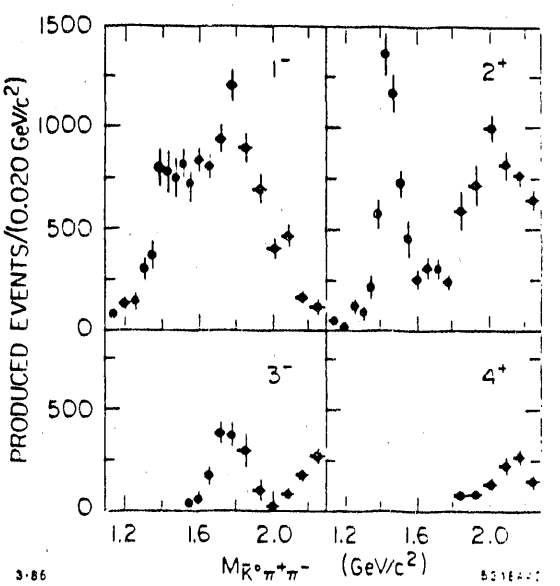

FIGURE 4
The natural spin-parity intensity distributions obtained from the amplitude analysis of reaction (1).

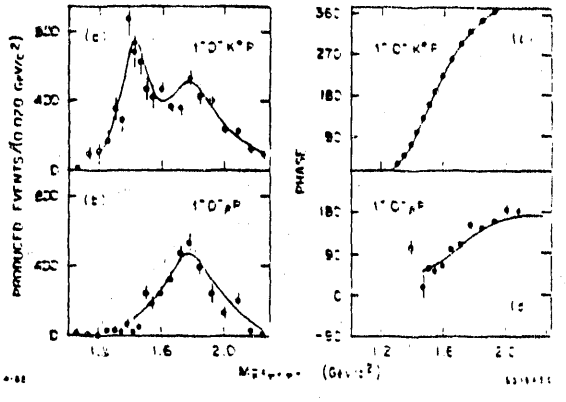

FIGURE 5
The individual isobar contributions to the 1^- distribution of Figure 4; the curves are described in ref. 14.

the $\overline{K^*}_2(1430)$, the $\overline{K^*}_3(1780)$ and the $\overline{K^*}_4(2060)$ are observed in the 2^+, 3^- and 4^+ distributions, respectively. The 2^+ distribution exhibits a second peak at ~ 2 GeV/c^2, while the 1^- distribution has a shoulder at ~ 1.4 GeV/c^2 followed by a peak at ~ 1.8 GeV/c^2. The $\overline{K^*}(892)\pi$ and $\overline{K}\rho(770)$ contributions to the 1^- spectrum are shown in Figures 5a,b; the curves result from a description in terms of two Breit-Wigner(BW) resonances. The lower mass state (M=1420±17, Γ=240±30 MeV/c^2) approximately decouples from the $K\rho$ channel, and its production characteristics indicate weak coupling to $K\pi$ also; it is most readily interpreted as the first radial excitation of the $\overline{K^*}(892)$. The second state (M=1735±30, Γ=423±48 MeV/c^2) may be the underlying member of the ^{3}D ground state; however its mass is greater and its width significantly larger than that obtained from reaction (2)[15] so that it could be a mixture of this state and the second radial excitation of the $\overline{K^*}(892)$.

A similar fit to the 2^+ data yields mass and width estimates of 1973 ± 33 and 373 ± 93 MeV/c^2 respectively for the higher mass state, which corresponds most probably to the first radial excitation of the $\overline{K^*}(1430)$,[14] although it may also be a partner to the $\overline{K^*}_4(2060)$ in the F wave ground state triplet.

The raw $K^-\pi^+$ mass spectrum for reaction (2) is shown in Figure 6; the shaded region corresponds to events with M(n π^+)≥ 1.7 GeV/c^2. In addition to an elastic BW amplitude describing the $\overline{K^*}(892)$ (cf.Figure 10), the amplitude analysis[15] yields the resonant D-H wave signals of Figure 7, thereby extending the observed leading orbital states to $J^P = 5^-$. The corresponding behavior of the underlying S wave amplitude up to 1.6 GeV/c^2 is shown in Figure 8. The curves correspond to an effective range parametrization plus a BW amplitude (M=1412 ± 4 ± 5, Γ=294 ±10 ±21 MeV/c^2), and the resultant S wave is approximately elastic up to ~ 1.5 GeV/c^2. The state described by the BW is the $^3P_0$ partner of the $\overline{K^*}(1430)$. Above 1.8 GeV/c^2, there are two S wave solutions, as shown in Figure 9. Both resonate in the 1.9-1.95 GeV/c^2 region, have width ~ 0.2 GeV/c^2 and elasticity ~ 0.5. In the quark model such a state can only be the first radial excitation of the $^3P_0$ ground state.

Finally, the behavior of the P wave $\overline{K}\pi$ scattering amplitude from reaction (2) is shown in Figure 10 for the region up to 1.8 GeV/c^2. The solid curve provides a satisfactory description in terms of three BW resonances:[15] (i) the $\overline{K^*}(892)$; (ii) a resonance at ~ 1.4 GeV/c^2 of elasticity ~ 0.07 which is consistent with the radial excitation of the $\overline{K^*}(892)$ observed in reaction (1); and (iii) a resonance (M=1677 ±10 ±32, Γ=205 ±16 ±34

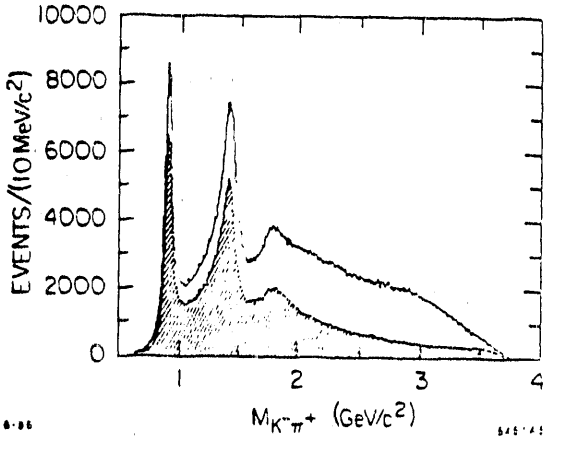

FIGURE 6
The raw $K^-\pi^+$ mass distribution for reaction (2); the shaded region corresponds to events with M(n π^+) ≥ 1.7 GeV/c^2.

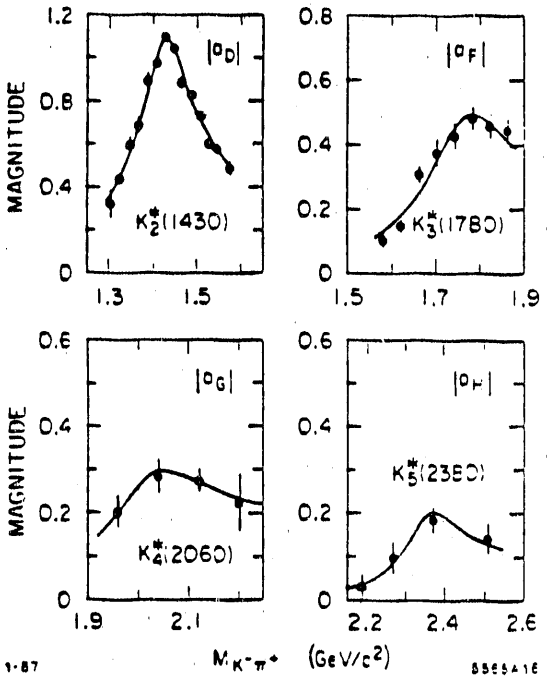

FIGURE 7
The mass dependence of the amplitudes of the leading orbital states obtained from reaction (2).

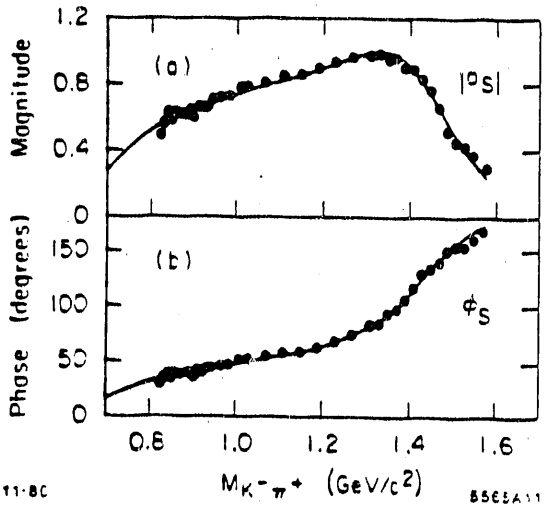

FIGURE 8
The behavior of the S wave $\overline{K}\pi$ scattering amplitude up to 1.6 GeV/c² from reaction (2); the curves are described in ref.15.

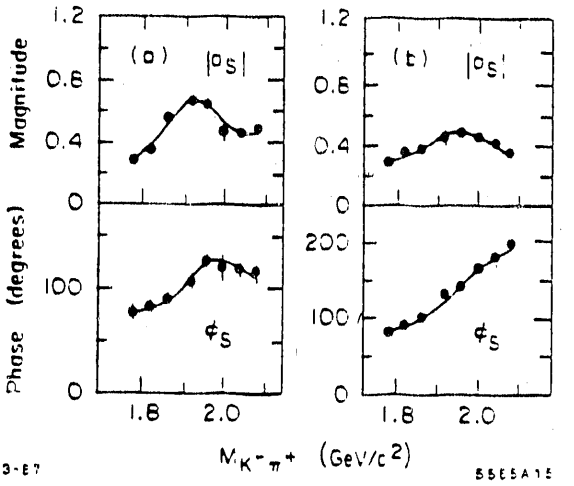

FIGURE 9
The behavior of the S wave $\overline{K}\pi$ scattering amplitude solutions above 1.8 GeV/c² from reaction (2); the curves are described in ref.15.

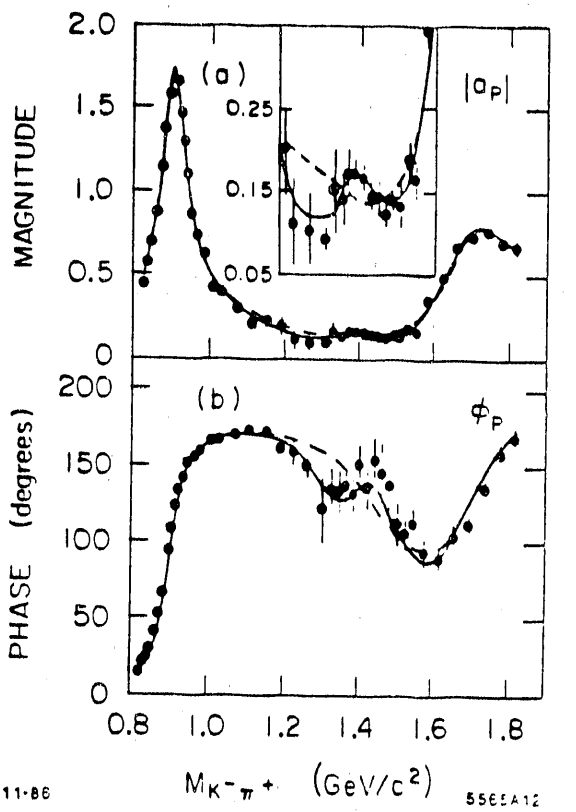

FIGURE 10
The behavior of the P wave $\overline{K}\pi$ scattering amplitude up to 1.8 GeV/c² from reaction (2); the curves are described in ref.15.

MeV/c^2) of elasticity $\sim$ 0.39 which is readily interpreted as the $^3D_1$ ground state.

The production mechanism for reactions (1) and (2) is predominantly unnatural parity, helicity zero exchange. In contrast, the $\overline{K}^0\pi^-$ system in reaction (3)[16] is produced mainly by natural parity, helicity one exchange (cf. Figure 11). Nevertheless, a description of the mass dependence of the resulting amplitude and phase data requires the same P, D and F wave resonance structure found for reactions (1) and (2). This is illustrated in Figure 12, where the solid curves correspond to three P wave resonances, two D wave resonances, and one F wave resonance. Clearly, these structures are required in order to reproduce the relative phase motion, and the parameter values obtained from reaction (3) agree well with those obtained from reactions (1) and (2).

Reaction (4) has been measured with large statistics for the first time in the present experiment, and the resulting $K^-\eta$ mass spectrum is shown in Figure 13. An amplitude analysis of the $K^-\eta$ system[17] has established that the peak at $\sim$1.8 GeV/c^2 results from production of the $\overline{K}^*_3(1780)$ (cf.Figure 14). This, together with the results of a similar analysis of reaction (3),[16] yields a branching fraction to $\overline{K}\eta$ of 7.7$\pm$1.0%, in accord with SU(3). SU(3) predicts also that K^* states of even spin couple only weakly to $K\eta$. This is confirmed by the D wave intensity distribution of Figure 14. No $\overline{K}^*_2(1430)$ signal is observed, and a 95% confidence level upper limit on the branching fraction is established at 0.45%. This value is an order of magnitude smaller than that obtained from previous low statistics measurements. A further implicationof this result is that 0^+ K^*s should couple only weakly, if at all, to the $K\eta$ channel. This is consistent with the observation (Figure 8) that the S wave $K^-\pi^+$ scattering amplitude appears to be purely elastic up to $\sim$ 1.5 GeV/c^2, which is well beyond $K\eta$ threshold.

4. SYSTEMATICS OF THE LEVEL STRUCTURE

A general feature of Figure 2 is that the level structure appears to depend in first approximation only on principal quantum number value; i.e. there is approximate mass degeneracy of states having different spin-

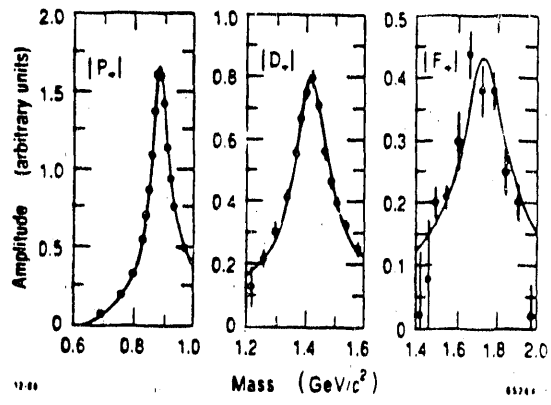

FIGURE 11
The mass dependence of the leading $\overline{K}^*$ amplitudes from reaction (3); the subscript indicates that production is via helicity one natural parity exchange in the t channel.

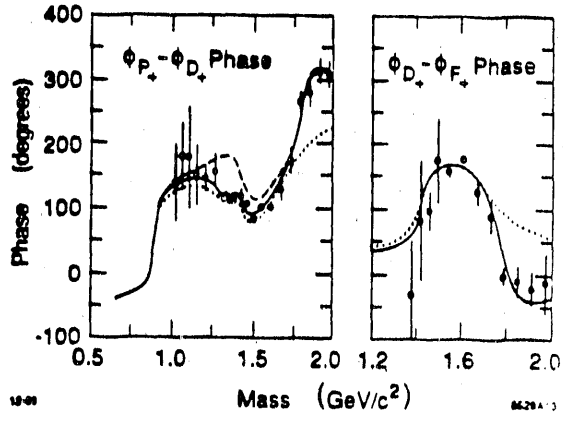

FIGURE 12
The mass dependence of the relative phase between the P-D and D-F amplitudes of figure 11; the solid curves are described in the text; the dotted curve is obtained if the second D wave resonance is excluded; the dashed curve is obtained if the small P wave resonance at $\sim$ 1.4 GeV/c^2 is excluded.

parity but the same value of the (orbital+radial) excitation quantum numbers. A notable exception involves the S wave ground states; this suggests that the spin-spin interaction is large only in this configuration.

The leading orbital excitations lie on almost degenerate Regge trajectories. However, the trajectory slope appears to differ for the natural and unnatural parity states, being 0.8-0.85 (GeV/c^2)$^{-2}$ for the former, and

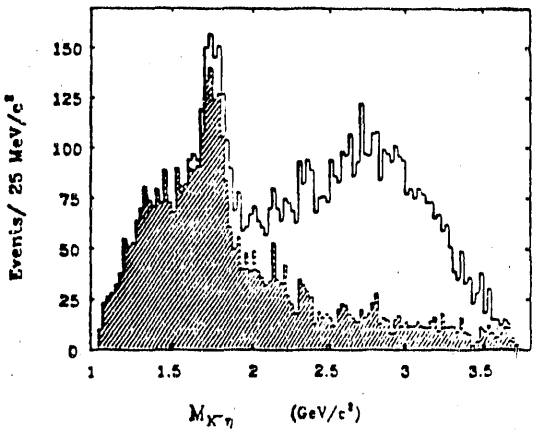

FIGURE 13
The $K^-\eta$ mass distribution from reaction (4); the shaded region corresponds to M(ηp)$\geq$ 2.0 GeV/c^2 and M(K^-p) $\geq$ 1.85 GeV/c^2.

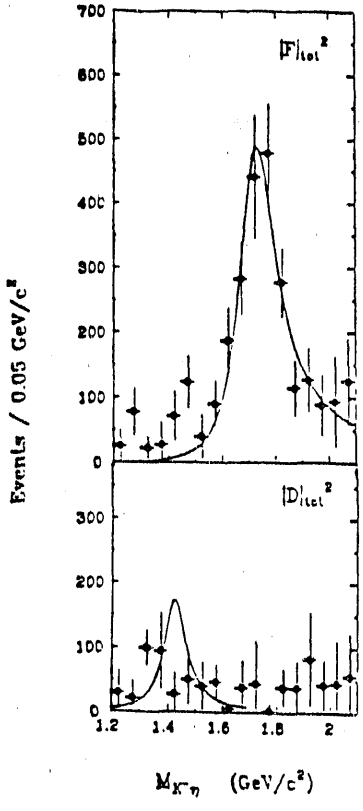

FIGURE 14
The total F and D wave intensity distributions from reaction (4); the F wave curve corresponds to a $\overline{K^*}_3$ (1780) BW; the D wave curve indicates the 95% confidence level limit on $\overline{K^*}_2$ (1430) production.

0.65-0.7 (GeV/c^2)$^{-2}$ for the latter. A consequence of this difference is that the relative level structure in the ground state triplets changes with increasing mass such that the unnatural parity state appears to move through the natural parity doublet (cf. Figure 2). This is indicative of a complicated spin-orbit interaction which may even be impossible to reproduce in the context of a potential model. In particular, the P wave triplet structure is very different from that observed for the χ_c or χ_b states. For the strange meson triplet, the $K_2^*(1430)$ and the $K_0^*(1410)$ are significantly higher in mass than the K_{1a} and the K_{1b}, which are the $q\bar{q}$ states extracted from the $K_1(1270)$ and the $K_1(1400)$. In contrast, mass decreases monotonically with J for the χ_c and χ_b states. It should be noted that a similar splitting pattern occurs in the isovector sector, where the $a_2(1320)$ and the $a_0(1320)$ are higher in mass than the $a_1(1260)$ and the $b_1(1235)$; indeed the overall level structure for the isovector sector[3] is rather similar to that of Figure 2.

The calculations of ref.1 indicate that the splittings in mass of the radially excited states with respect to the ground states should be much the same for the strange, $c\bar{c}$ and $b\bar{b}$ mesons, and in this respect the predictions are in rough agreement with the data of Figure 2. However, the $^3P_0$ ground state is predicted $\sim$ 170 MeV/c^2 low, and the $^3S_1$ first radial excitation is predicted $\sim$ 160 MeV/c^2 high with respect to the corresponding measured mass value. Also, for the $^3S_1$ and $^3P_0$ levels the expected splitting between the ground state and first radial excitation is $\sim$650-680 MeV/c^2, whereas it is observed to be $\sim$500-550 MeV/c^2. It should be noted also that for the $^3S_1$ states this splitting is predicted to increase from the charmonium to strange meson sector; it appears actually to decrease by $\sim$70 MeV/c^2.

The $K_1^*(1410)$ and $K_0^*(1950)$ radially excited states exhibit very different elasticities ($\sim$ 0.07 and $\sim$ 0.5, respectively). This may be due to the different nodal structure of the radial wave functions describing the relevant $K\pi$ final states (cf. e.g. the L=0 and L=1 wave functions describing the first radial excitations of the hydrogen atom). Such features should be properly reproduced in any model describing the level structure, as should the apparent lack of coupling of the $K_1^*(1410)$ to

the $K\rho$ channel.

In summary, although a potential model such as that of ref.1 seems to be in qualitative agreement with the level structure of Figure 2, there would appear to be several areas which are quantitatively unsatisfactory. It would therefore be of interest to attempt to adjust the parameters of such a model in order to learn the extent to which these discrepancies can be removed within such a framework.

5. CONCLUSION AND FUTURE

A great deal has been learned about the spectroscopy and couplings of the strange meson states. The systematics agree quite well with quark model expectations, and, in particular, there is no evidence for the existence of "extra" states. However, as discussed in section 4, there are several puzzling features of the detailed structure which may not even be describable in the context of potential models.

On the experimental side, the LASS experiment has demonstrated:

(i) the effectiveness of a programmatic approach to the study of meson spectroscopy;

(ii) the feasibility of obtaining very large statistics in a fixed target experiment by running a 4π acceptance spectrometer in interaction mode;

(iii) that the corresponding computing requirements can be met by means of a combination of large mainframe and microprocessor farm availability;

(iv) that the resultant large data samples for individual reactions can be analyzed in a relatively straightforward manner;

(v) the value of being able to analyze many different channels in the same experiment under conditions of uniform and well-understood acceptance;

(vi) that such a program need not involve a large number of physicists and graduate students.

In the next ten years, it would be desirable to push such a program to a significantly higher statistical level, while maintaining the uniform acceptance which characterizes the LASS experiment. This would imply an experiment of something like five billion triggers. Such experiments are already contemplated at Fermilab, (e.g. E791) and it seems that the data processing, storage and retrieval needs can be met. The level structure of Figure 2 would be significantly refined by such a program, and that in the strangeonium sector would be carried well beyond the present-day understanding of the strange sector. In addition, a programmatic study using pion beams should be carried out in order to similarly advance the understanding of the isovector and non-$s\bar{s}$ sectors.

The most likely place for such a program to come into being on the indicated time-scale is at TRIUMF by means of the KAON Factory project. The present plans call for an r.f. separated beam line in the 6-20 GeV/c range providing $\sim 10^7$ K's per spill. The lab. is contemplating a spectrometer facility which is something of a cross between LASS and the Crystal Barrel detector at LEAR. Furthermore, this spectrometer facility figures prominently in the planned program of the lab., thereby indicating strong in-house commitment. There appears to be enthusiasm for such a facility among the user community, and development of the necessary computing capabilities of the lab. is being considered.

The programmatic approach to the study of meson spectroscopy over the last twenty years or so at SLAC has proven its worth. However, there is much that remains to be understood, and it would seem that this greater understanding can only be achieved by means of the higher level, long-term program embodied in KAON, and consequently that the future of the subject is intimately bound to the approval and construction of this facility.

REFERENCES

1. S. Godfrey and N. Isgur, Phys. Rev. D32 (1985) 189.
2. W. Grotrian, Graphische Darstellung der Spektren von Atomen und Ionen mit ein, zwei und drei Valenzelektronen (Springer, Berlin, 1928).
3. Particle Data Group, Phys. Lett. 239B (1990).
4. T. Armstrong et al., Nucl. Phys. B221 (1983) 1.
5. D. Frame et al., Nucl. Phys. B276 (1986) 667.

6. W. Cleland et al., Nucl. Phys. B184 (1981) 1.
7. T. Armstrong et al., Nucl. Phys. B227 (1983) 365.
8. M. Baubiller et al., Nucl. Phys. B183 (1981) 1.
9. S.U. Chung et al., Phys. Lett. 51B (1974) 413.
10. C. Daum et al., Nucl. Phys. B187 (1981) 1.
11. G. Brandenburg et al., Phys. Rev. Lett. 26 (1976) 703.
12. D. Aston et al., The LASS Spectrometer, SLAC-REP-298 (1986).
13. D. Aston et al., Nucl. Phys. B301 (1988) 525.
14. D. Aston et al., Nucl. Phys. B292 (1987) 693.
15. D. Aston et al., Phys. Lett. 180B (1986) 308; Nucl. Phys. B296 (1988) 493.
16. P.F. Bird, Ph.D. Thesis, SLAC Report 332 (1988).
17. D. Aston et al., Phys. Lett. 201B (1988) 169.

DISCLAIMER

END

DATE FILMED

01 / 28 / 91